

A SIMPLE TRANSIENT APPROACH TO MEASURING THERMAL CONTACT CONDUCTANCE AT LOW CONTACT PRESSURES

Matt Lenahan^{1*}, Andrew K. Owen¹, David R.H. Gillespie¹

¹Oxford Thermofluids Institute, Osney Mead, Oxford, OX2 0ES, UK

1. ABSTRACT

Limited data exists for thermal contact conductance h_c between surfaces which may contact lightly, such as differential thermal expansion at sealing faces. This paper describes a transient experimental technique to measure h_c between rough surfaces contacting at low pressures, allowing data to be gathered quickly and effectively using standard, simple apparatus. It produces comparable results to the bulk steady-state method several orders of magnitude faster, whilst being simple to implement, both physically and computationally. Overall measurement uncertainty is estimated in the range 0.40%-6.88% for $h_c = 100$ -100,000 W m⁻² K⁻¹.

2. INTRODUCTION

The simplest analyses of thermal contact conductance h_c at low pressures have been based on bulk steady-state methods^[1], which have the drawback of being very time-consuming. There exists a wide array of advanced methods, both steady-state and transient, of increasing complexity^[2]; however, there has thus far been no comprehensive transient treatment of the standard bulk steady-state apparatus, where a series of temperature measurements are used to infer the temperature drop at the interface ΔT_c , from which h_c is estimated via the relationship $q = h_c \Delta T_c$ (Figure 1). This would preserve the simplicity of the conventional approach while greatly reducing experimental time, as there would be no requirement to wait for steady-state to be established. The inverse transient problem of recovering an unknown parameter from measured temperatures is ill-posed due to its sensitivity to noise. At low contact pressures, the low h_c means that the temperature drop across the interface is much greater than the noise inherent to thermocouple measurements, and a simple transient method can produce accurate results. This work proposes and validates a predictor-corrector approach adapted from the function specification method^[3,4,5]. Preliminary data for h_c vs. applied pressure is presented based on application in gas turbine seals, with materials typical of shaft and seal components.

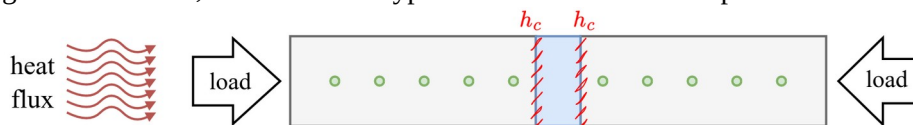


Figure 1. Schematic of the standard bulk steady-state apparatus; thermocouples in green.

3. METHODOLOGY

There are two components to the solver: a 1D, transient, direct solver, which uses a standard tri-diagonal matrix method with adjustments to allow for a specified h_c at an interface, and an inverse solver adapted from the function specification method. An initial value of the parameter of interest (h_c) is selected, then the direct solver is used to calculate the temperature distribution r steps into the future based on this value (the *prediction*). These temperatures are compared to the measured temperatures at the sensor locations, and the error is minimised to select the next h_c (the *correction*). This process is repeated until convergence. The use of r time steps provides resilience to noisy input data. The residual sum of squares between the measured temperatures Y and predicted temperatures \hat{T} is chosen as the objective function E , summed over s sensor locations and r time steps, beginning at the current time m . h_c is assumed constant over the r steps (this is the “function

*Corresponding Author: matthew.lenahan@stcatz.ox.ac.uk

specification"; a different function, such as a linear extrapolation, could be chosen). Since the procedure can be applied to multiple interfaces simultaneously, subscript k denotes the interface.

$$E_k = \sum_{j=1}^s \sum_{i=1}^r \left[Y_{j,m+i-1} - \hat{T}_{j,k,m+i-1}(h_{k,m+i-1}) \right]^2 \approx \sum_{j=1}^s \sum_{i=1}^r \left[Y_{j,m+i-1} - \hat{T}_{j,k,m+i-1}(h_{k,m}) \right]^2 \quad (1)$$

The $(j, k, m+i-1)^{th}$ sensitivity coefficient, the sensitivity of the calculated temperature \hat{T} to change in the parameter of interest h_c , is defined as

$$X_{j,k,m+i-1} = \frac{\partial \hat{T}_{j,k,m+i-1}(h_{k,m})}{\partial h_{k,m}} \approx \frac{\hat{T}_{j,k,m+i-1}(h_{k,m} + \epsilon h_{k,m}) - \hat{T}_{j,k,m+i-1}(h_{k,m})}{\epsilon h} \quad (2)$$

where ϵ is a small number. The increment on $h_{k,m}$ for the p^{th} iteration of Newton's method, $\Delta h_{k,m}^p$, is given by

$$\Delta h_{k,m}^p = \frac{\sum_{j=1}^s \sum_{i=1}^r \left(Y_{j,m+i-1} - \hat{T}_{j,k,m+i-1}(h_{k,m}^p + \epsilon h_{k,m}^p) \right) X_{j,k,m+i-1}^p}{\sum_{j=1}^s \sum_{i=1}^r \left[X_{j,k,m+i-1}^p \right]^2} \quad (3)$$

Convergence criteria are defined as relative change in h , relative change in E , and a maximum number of iterations. While the k^{th} h_c is calculated, all other h_c are held constant at their previous value. The minimum time step required for convergence of the direct solver is small, while the interval between experimental data is comparatively large, and not always constant (for example, if software timing is used for data acquisition). Therefore, two different time scales are required: a constant Δt satisfying the 1D stability criterion, and an integer counter for data referencing the time t_i at which the i^{th} measurement was taken. Temperature-dependent material properties are calculated at each step. After convergence, the direct solver is run once with the final values of the parameters from the current step to provide the initial temperature distribution for the next step.

The experimental procedure is as follows: the heat source is switched on and heat is allowed to propagate up the stack for a warm-up period t_w of at least the characteristic time scale for diffusion, until there is a significant temperature difference between the two thermocouples furthest from the source; data acquisition is started and the pressure held constant at its initial value for a settling time t_s , which is required for the inverse solver to iterate from an initial estimate of the temperature distribution to an accurate distribution; then pressure is varied in a stepwise manner, and the $h_c(t)$ recovered by the inverse solver is averaged across sections of constant pressure (hence constant h_c) to generate a single point of data \bar{h}_c corresponding to a single pressure p .

The method was validated using noisy, synthetic temperature data generated by the direct solver given an input stepwise $h_c(t)$ and temperature boundary conditions for the heat source and sink. A constant offset drawn from $N(\mu=0, \sigma=0.0270)$ was added to each sensor, and a random noise drawn from $N(\mu=0, \sigma=0.0358)$ was added to every measurement, representing thermocouple accuracy and thermal/electrical noise respectively. The noise models were based on steady-state room-temperature measurements from the ten thermocouples in the experimental setup. The inverse solver is then used to recover the input $h_c(t)$. Optimal values for the parameters $t_w, t_s, \Delta x$ and r were evaluated, then overall measurement uncertainty was calculated as the sum of trueness (deviation of the mean recovered \bar{h}_c from the input) and precision (the 95% confidence limit of Student's t-distribution).

4. RESULTS

Figure 2 shows the relative overall measurement uncertainty calculated from 20 sets of noisy, synthetic temperature data for h_c in the range 100-100,000 W m⁻² K⁻¹ representing the range of h_c expected at low contact pressure in air (higher than in a vacuum due to conduction in the air gap). Uncertainty ranges from 0.40% to 6.88%. For high h_c , uncertainty increases as ΔT_c becomes very small whilst noise in the temperature measurements remains constant, reducing signal-to-noise ratio. Similarly, for small h_c the solver's estimation of heat flux at the interface becomes susceptible to noise as the large ΔT_c results in a very small temperature

difference between neighbouring sensors, again increasing uncertainty in h_c (q is not explicit in the formulation, but implicit in the definition of h_c). The effect at low h_c is not so apparent in Figure 2, but is significant for h_c below $100 \text{ W m}^{-2} \text{ K}^{-1}$. Figure 3 shows some example data for h_c versus pressure gathered using the above method between nickel-chromium superalloy meter bars and a machine-turned specimen of alloy L605, selected to represent the rotor-seal interface of an aero-engine. An interesting hysteresis is observed compared to the experiments performed under vacuum in reference [1] due to the presence of a compressible fluid (air) at the interface.

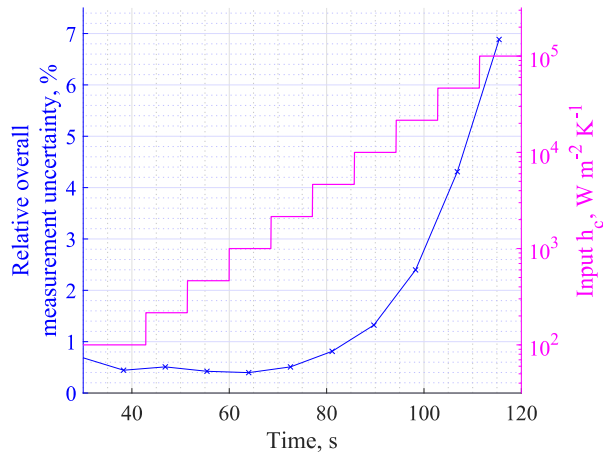


Figure 2. Relative overall measurement uncertainty (blue) calculated from 20 runs of the inverse solver on noisy, synthetic temperature for a stepwise input $h_c(t)$ (pink). Uncertainty varies with h_c due to signal-to-noise ratios: at high h_c , ΔT_c is very small, and at low h_c , temperature difference between neighbouring sensors is very small, whilst noise remains constant across the whole range.

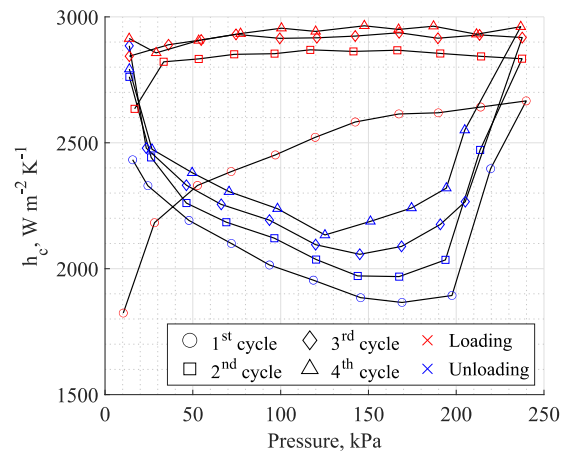


Figure 3. h_c versus pressure for interface between nickel-chromium superalloy meter bars and machine-turned specimen of alloy L605 gathered using the above method. Collecting and processing data took less than 2 hours.

5. CONCLUSIONS

The experimental method outlined above produces results with uncertainty comparable to the bulk steady-state method, without the need to wait for steady-state to be reached. It took less than 2 h to gather and process the 84 points of data in Figure 3; this compares favourably with the 12 h to produce a single point of data in reference [1]. Uncertainty varies with h_c , but the solver performs well for h_c in the range expected of low contact pressure in air. The preliminary data show expected behaviour on initial loading, which can be linked analytically to the surface asperity contact area between the surfaces and local surface conditions, as well as an interesting, repeatable hysteresis differing from the behaviour observed under vacuum. Further material pairs and surface properties, including other machined surfaces, surface oxide layers, and presence of oil, have been characterised, to be presented in future.

REFERENCES

- [1] F. H. Milanez, M. M. Yovanovich, and M. B. H. Mantelli, 2004, "Thermal contact conductance at low contact pressures." *Journal of Thermophysics and Heat Transfer* 18, No. 1, pp. 37-44.
- [2] Xian, Yaoqi; Zhang, Ping; Zhai, Siping; Yuan, Peng; and Yang, Dauguo; 2018, "Experimental characterization methods for thermal contact resistance: A review." *Applied thermal engineering* 130, pp. 1530-1548.
- [3] J. V. Beck, B. Blackwell, and C. R. St Clair Jr., 1985, *Inverse Heat Conduction: Ill-Posed Problems*, Wiley-Interscience.
- [4] G. Rauer, A. Kühhorn, and M. Springmann, 2014, "Residual stress modelling and inverse heat transfer coefficients estimation of a nickel-based superalloy disc forging." In *Proceedings of ASME Turbo Expo 2014: Turbine Technical Conference and Exposition*. ASME Paper No. GT2014-25827.
- [5] T. S. Kumar, 2004, "A serial solution for the 2-D inverse heat conduction problem for estimating multiple heat flux components", *Numerical Heat Transfer, Part B: Fundamentals*, 45:6, pp. 541-563